Journal of Thermal Analysis, Vol. 52 (1998) 975-983

EFFECTS ON THE THERMAL PROPERTIES AND BIOACTIVITY OF SUBSTITUTION OF CaO BY M_2O_3 (*M*=La, Y, Al) IN WOLLASTONITE GLASS

A. Costantini, F. Arcobello Varlese, A. Buri and F. Branda

Dipartimento di Ingegneria dei Materiali e della Produzione, Università 'Federico II', Napoli, Italy

Abstract

The effects on the thermal properties and bioactivity of the substitution of CaO by La_2O_3, Y_2O_3 and Al_2O_3 in a glass of composition $CaO{\cdot}SiO_2$ were studied and compared. The trivalent metal oxides were all effective in raising the glass transformation and softening temperatures when they replaced CaO in the glass of composition $CaO{\cdot}SiO_2$. The experimental results suggest that Al_2O_3 plays the role of a glass-former, while La_2O_3 and Y_2O_3 behave as glass-modifiers. The tendency to devitrify appears to be the lower, the farther the glass composition is from those of the crystalline phases, owing to the need for diffusion over longer distances, the greater the composition difference. The substitution with the trivalent metal oxides is detrimental to the bioactivity, which is preserved only in the event of very small degrees of substitution. The most negative role appears to be played by Al_2O_3.

Keywords: bioactivity, glass structure, glass transformation temperatures, non-isothermal crystallization, substituted (Al, Ga, Y) calcium silicates

Introduction

CaO and SiO_2 are the basic components of bioactive glasses and glass-ceramics, i.e. ceramics able to bond to living bone [1–4] and are of great interest for the repair and reconstruction of diseased or damaged parts of the musculo-skeletal system [1–4]. It is also known that the addition of La_2O_3 and Y_2O_3 to silicates results in glasses with high elastic moduli and hardness [5].

In this paper, the effects on the thermal properties and bioactivity of the substitution of CaO by La_2O_3, Y_2O_3 and Al_2O_3 in a glass of composition $CaO{\cdot}SiO_2$ have been studied and compared.

Experimental

Glasses of composition

$$(2-x)CaO{\cdot}x/3M_2O_3{\cdot}2SiO_2 \qquad 0\leq x\leq 1.0 \qquad (M=Y, La) \qquad (1)$$

$$(2-x)CaO{\cdot}xAl_2O_3{\cdot}2SiO_2 \qquad 0\leq x\leq 1.0 \qquad (2)$$

1418–2874/98/ $ 5.00

Akadémiai Kiadó, Budapest

Kluwer Academic Publishers, Dordrecht

were prepared by melting analytical grade reagents $CaCO_3$, Y_2O_3, La_2O_3, Al_2O_3 and SiO_2 in a platinum crucible in an electric oven for 4 h in the temperature range 1400–1600°C. The melts were quenched by plunging the bottom of the crucible into cold water.

Differential thermal analysis (DTA) was carried out with a Netzsch heat flux differential scanning calorimeter (DSC) model 404 M on about 50 mg powdered samples at a heating rate of 10°C min^{-1}. Finely powdered (+63–90 μm) samples were used. Powdered Al_2O_3 was used as reference material.

In order to study the bioactivity, as done by other researchers [4], samples of the studied glasses were soaked in a simulated body fluid (SBF) with a composition nearly identical to that of human blood plasma, as reported in the literature. The SBF solution was buffered at pH=7.25; during soaking, the temperature was fixed at 37°C. The ability to form an apatite layer was studied by submitting reacted samples to infrared (IR) spectroscopy. Powders (–170+230 mesh) were produced with an average surface area of $5.9 \cdot 10^{-3}$ mm^2. They were soaked in SBF and analysed by IR spetroscopy. Since the ratio of the exposed surface to the volume of solution influences the reaction [6, 7], a constant ratio of 50 mm^2 ml^{-1} of solution was applied. This corresponds to the value previously used to study the bioactivity of $CaO \cdot SiO_2$ glasses [4].

Fourier transform infrared (FTIR) transmittance spectra were recorded in the range 400–1200 cm^{-1}, using a Mattson 5020 system, equipped with a DTGS KBr (deuterated triglycine sulphate with potassium bromide windows) detector, with a resolution of 2 cm^{-1} (20 scans). KBr pelletized disks containing 2 mg of sample and 200 mg KBr were made. The FTIR spectra were processed by means of Mattson software (FIRST Macros).

Results and discussion

Thermal properties

The recorded DTA curves are similar to those published elsewhere [8]. After the first slope change in the glass transformation range, a second one appears in the curve before the devitrification exo-peak. It is due to the variation in the heat-transfer coefficient that occurs when the sample softens and wets the sample-holder walls. The temperatures of glass transformation, T_g, and softening, T_s, were taken as the inflection and the onset points, respectively, of the described effects.

Figures 1 and 2 show plots of the glass transformation, T_g, softening, T_s, and exo-peak, T_p, temperatures *vs.* the glass composition expressed by means of the values of x in formulae (1) and (2).

Figure 1 reveals both linear and non-linear plots of T_g *vs.* composition. In the composition range $0 \leq x \leq 0.6$, Y_2O_3 is the most effective of the three oxides in increasing T_g. At greater degrees of substitution ($x \geq 0.6$), Al_2O_3 is the most effec-

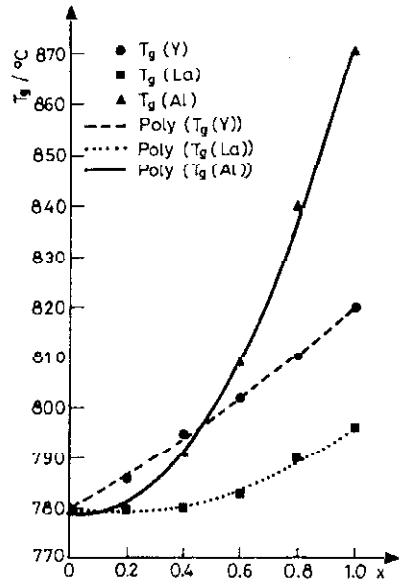

Fig. 1 Glass transformation temperature, T_g, *vs.* composition

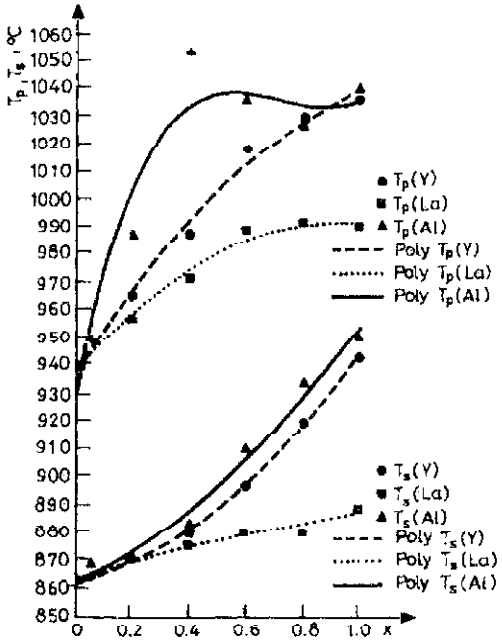

Fig. 2 Softening, T_s, and devitrification exo-peak, T_p, temperatures *vs.* composition

tive. This latter result is partly due to the different substitution ratio M_2O_3/CaO, which is higher in the case of Al_2O_3. The different kinds of plot can be related to the different roles of the added oxides. The role of an intermediate oxide played by Al_2O_3 is well established [9]. In the presence of a glass-former, such as SiO_2, it is able to form AlO_4 tetrahedra, whose negative charge, however, needs to be compensated by the presence of a modifier oxide. As a consequence, CaO is reduced to its usual depolymerizing effect, i.e. the breaking of Si–O–Si bridges: when Al_2O_3 is present, the oxygen atoms added as CaO are taken up to construct the AlO_4 tetrahedra and the Ca^{2+} ions play the role of charge compensators. When the molar ratio $CaO/Al_2O_3=1$, all the CaO is devoted to its depolymerizing role and a structure similar to the SiO_2 one is obtained. Following Ray [10], the increase in density of covalent cross-linking makes T_g increase, just as observed in Fig. 1. The non-linear trend is also similar to those observed in the case of alkali metal silicate glasses containing glass forming trivalent oxides [11].

Table 1 Ionic radii, R [Å], and ionic field strengths, Z/R^2, [$Å^{-2}$] of cations

Cation	R	Z/R^2
Ca^{2+}	0.99	2.04
Y^{3+}	0.89	3.76
La^{3+}	1.14	2.3

In contrast, Y_2O_3 and La_2O_3 are classified as network modifier oxides [9]. In this hypothesis, when CaO is substituted by them in a molar ratio $CaO/M_2O_3=3$, no change in covalent cross-linking density is expected. Therefore, following Ray [10], the T_g changes are related to the differences in number and strength of the bonds of the modifier ions with the oxygens. It has been shown that the effect of bond strength can be described on the basis of the ionic field strength [12, 13], which is defined as the ratio of the ionic charge to the square of the radius of the cation. Table 1 reports the ionic field strengths and the radii of the modifier ions. The T_g increase recorded when Y_2O_3 is substituted for CaO can be related to the greater field strength of Y^{3+}. The slight increase induced by La_2O_3 can be attributed to the greater ionic radius of La^{3+}, whose mean coordination number should therefore be greater than that of Ca^{2+}. The non-linearity trend recorded in this case can be ascribed, as already proposed for other glassy compositions [13], to a 'difficulty', at the beginning of the substitution, in creating its own coordination when a modifier cation is substituted for another of close ionic field strength.

The increasing trends in the T_s curves reported in Fig. 2 can be explained in a similar way. In order to discuss the T_p curves, it is useful to plot (as in Fig. 3) the difference between the peak and glass transformation temperatures, T_p-T_g *vs.* the composition, and discuss this diagram in the light of the crystalline phases re-

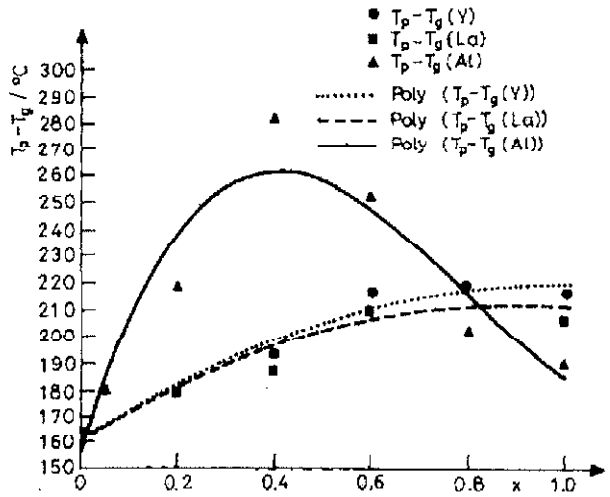

Fig. 3 Plot of the difference between the devitrification peak, T_p, and glass transformation, T_g, temperatures *vs.* composition

ported in Table 2, formed when devitrification occurs. The glass compositions of the end-terms of the Al_2O_3 series correspond to those of crystalline wollastonite, $CaO{\cdot}SiO_2$, and anortite, $CaO{\cdot}Al_2O_3{\cdot}2SiO_2$, which effectively are found to form during non isothermal crystallization. In the La_2O_3 and Y_2O_3 series, this is true only for x=0. In fact, in this case, the XRD patterns (not reported) of the devitrified x=1 sample show evidence of a residual glassy phase besides the reflections reported in Table 3, which could not be attributed to any phase reported in the JCPDS cards. Since the difference T_p–T_g can be related to the tendency to devitrify, being greater the difficulty in crystallization, the trends of the plots reported in Fig. 3 can be explained: the difference grows on moving from the com-

Table 2 Crystalline phases formed during non-isothermal crystallization

x	Al_2O_3 series	La_2O_3 series	Y_2O_3 series
0	wollastonite	wollastonite	wollastonite
0.2	wollastonite pseudowollastonite	wollastonite pseudowollastonite	wollastonite unknown phase 2
0.4	wollastonite pseudowollastonite anortite	wollastonite pseudowollastonite unknown phase 1	wollastonite unknown phase 2
0.6	wollastonite anortite	wollastonite pseudowollastonite unknown phase 1	wollastonite unknown phase 2
0.8	anortite	unknown phase 1	unknown phase 2
1.0	anortite	unknown phase 1	unknown phase 2

Table 3 *d*-spacings and relative intensities of the lines of the diffraction patterns indexed as unknown phases 1 and 2 in Table 2 (s=strong; w=weak)

Unknown phase 1		Unknow phase 2	
d-spacing/ Å	relative intensity	*d*-spacing/ Å	relative intensity
3.045	s	3.09	s
2.494	w	2.53	w
2.487	w	2.50	w
2.222	w	2.25	w
1.931	ww	1.90	w
1.920	w		
1.631	ww		
1.626	ww		

position of a crystalline phase, because of the need for diffusion over longer distances, the greater the difference from the composition of the crystalline phase; the maximum in the curve of the Al_2O_3 series can be explained by the fact that both the end-term compositions corresponds to one of a crystalline phase.

Bioactivity

It is well established in the literature that the essential condition for glasses and glass-ceramics to bond to living bone is the formation of a hydroxyapatite layer on their surfaces in the body [1–4]. 'In vitro' bioactivity tests are conducted by dipping the studied samples in an SBF [1–4].

The FTIR spectra of samples treated as reported in the Experimental section are reported in Figs 4 and 5. In particular, Fig. 4 reports FTIR spectra of $CaO{\cdot}SiO_2$ samples as-quenched and after a 3-day soaking in SBF, together with those relative to the glass x=0.2 in the La_2O_3 series. The spectra of the corresponding glasses in the Y_2O_3 and Al_2O_3 series are similar and are not reported. They were interpreted on the basis of the peak assignments suggested in the literature for other bioactive glasses [4, 6]. The as-quenched spectra display a broad band in the frequency range 800–1100 cm^{-1} and a band at about 470 cm^{-1}. The spectra are consistent with those reported in the literature [14] for alkali metal and alkaline earth silicates. The band in the range 800–1100 cm^{-1} is ascribed to the stretching modes of SiO_4 tetrahedra. It is broader when the content of the modifier oxide is greater. In fact, an increase of the modifier oxide content involves the occurrence of SiO_4 tetrahedra with a progressively greater number of non-bridging oxygens and, therefore, the extension of the absorption band to lower frequencies [14, 15]. As concerns the band at 470 cm^{-1}, it is ascribed to the

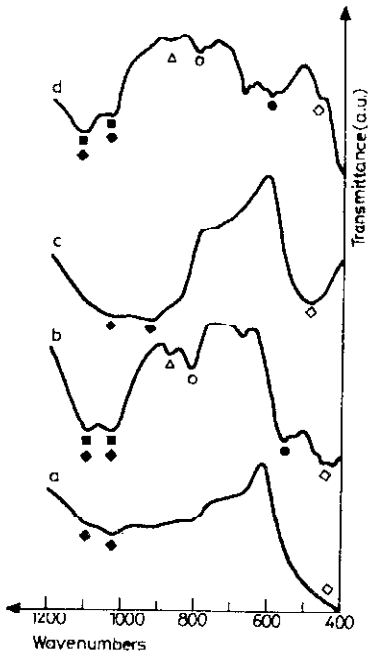

Fig. 4 FTIR spectra: of $1.8CaO{\cdot}0.2/3La_2O_3{\cdot}2SiO_2$ as-quenched (a) and after a 3-day soaking in SBF (b) and of $CaO{\cdot}SiO_2$ as-quenched (c) and after a 3-day soaking in SBF (d); ♦ – Si–O stretching; ◊ – Si–O–Si– bending; ○ – Si–O–Si– bond vibration between two SiO_4 tetrahedra; ■ – P–O stretching; • – P–O bending; △– C–O stretching

Si–O–Si bending mode [15]. Figure 4 suggests that initially major compositional and structural changes occur at the surface of the glass. The band (800–1100 cm^{-1}) becomes progressively sharper and a new band appears at 800 cm^{-1} which can be assigned to the Si–O–Si band vibration between two adjacent tetrahedra and is reported to be characteristic of silica gel [15]. According to the mechanism reported in the literature [1, 2], a silica gel layer is observed to form as a result of the cation-exchange, hydrolysis and polycondensation reaction. The appearance of a band at 580 cm^{-1} after different soaking times can be assigned [15] to the P–O bending vibration mode of a PO_4 group in a PO_4 tetrahedron, and indicative of the formation of a calcium phosphate layer. Its splitting into two peaks at 600 and 560 cm^{-1} is reported to be characteristic of hydroxyapatite crystals [15]. The 1116 and 1035 cm^{-1} bands, usually assigned to P–O stretching [15], are superimposed on the bands relating to the Si–O stretching mode and are not clearly distinguishable. A phosphate-rich layer therefore begins to form during the 3-day soaking, and afterwards continues to develop, as indicated by the 7-day soaking results reported in Fig. 6. However, only in the case of $CaO{\cdot}SiO_2$ and of the x=0.2 glass in the La_2O_3 series is evidence of the forma-

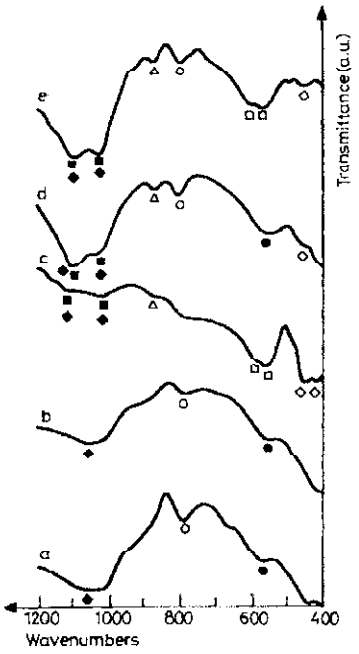

Fig. 5 FTIR spectra of 7-day soaked samples of 1.95 $CaO{\cdot}0.05Al_2O_3{\cdot}2SiO_2$ (a), $CaO{\cdot}SiO_2$ (e) and $1.8CaO{\cdot}0.2/3M_2O_3{\cdot}2SiO_2$ (M=Al (b), La (c) and Y (d)). Symbols as in Fig. 4

tion of crystalline hydroxyapatite obtained. The unreported FTIR results relative to M_2O_3-richer samples soaked in SBF show no signs of a calcium phosphate layer, even after a 7-day dipping. Therefore, the addition of the trivalent metal oxides is detrimental to the bioactivity, which is preserved only in the event of very small degrees of substitution. However, Fig. 5 suggests that the most negative role is played by Al_2O_3. In order to establish whether this could be due to the differences in the concentrations of CaO and trivalent metal oxide, a glass of composition $1.8CaO{\cdot}2/3Al_2O_3{\cdot}2SiO_2$, i.e. close to the composition of the x=0.2 glasses in the La_2O_3 and Y_2O_3 series, was prepared and tested. The results, also reported in Fig. 5, confirm the above deduction.

Conclusions

These trivalent metal oxides are all effective in raising the glass transformation and softening temperature when they substitute CaO in the glass of composition $CaO{\cdot}SiO_2$. The experimental results suggest that Al_2O_3 plays the role of glass-former, while La_2O_3 and Y_2O_3 behave as glass-modifiers. The tendency to devitrify appears to become lower, the farther the glass composition is from those of the crystalline phases, owing to the need for diffusion over longer distances, the greater the composition difference. The substitution of the trivalent

metal oxides is detrimental to the bioactivity, which is preserved only in the event of very small degrees of substitution. The most negative role appears to be played by Al_2O_3.

References

1 L. L. Hench, J. Am. Ceram. Soc., 74 (1991) 1487.
2 T. Kokubo, Bol. Soc. Esp. Ceram. Vid. (Proc. XVI Int. Cong. Glass, Madrid, Vol. 1) 31-C 1 (1992) 119.
3 T. Kokubo, J. Non-Cryst. Solids, 120 (1990) 138.
4 C. Ohtsuki, T. Kokubo and T. Yamamuro, J. Non-Cryst. Solids, 143 (1992) 84.
5 A. Makishima, Y. Tamura and T. Sakaino, J. Am. Ceram. Soc., 61 (1978) 247.
6 L. L. Hench and D. E. Clark, J. Non-Cryst. Solids, 28 (1978) 83.
7 A. Paul ed.: Chemistry of glasses, second edition, Chapman and Hall. London, New York, 1990, p. 184.
8 F. Branda, A. Costantini, A. Buri and A. Tomasi, J. Thermal Anal., 41 (1994) 1479.
9 H. Rawson, Inorganic Glass Forming Systems. Academic Press, London & New York, 1967 p. 24.
10 N. H. Ray, J. Non-Cryst. Solids, 15 (1974) 423.
11 F. Branda, A. Buri, D. Caferra and A. Marotta, Phys. Chem. Glasses, 22 (1981) 68.
12 A. Buri, D. Caferra, F. Branda and A. Marotta, Phys. Chem. Glasses, 23 (1982) 37.
13 F. Branda, A Buri, D. Caferra and A. Marotta, J. Non-Cryst. Solids, 54 (1983) 193.
14 I. Simon and H. O. McMahon, 'Study of some binary silicate glasses by means of reflection in Infrared' J. Am. Cer. Soc., 36 (1953) 160.
15 Y. Kim, A. E. Clark and L. L. Hench, J. Non-Cryst. Solids, 13 (1989) 195.